Comparing Rectangular and Trapezoidal Seals Using the Finite Element Method

MICHEL F. KHURI AND EGONS TONS

To design proper seals, it is important to understand seal behavior and joint and crack geometry. Different seal cross sections are compared, namely, rectangular, trapezoidal, and trapezoidal-rectangular shapes. After a closed-form solution could not be achieved using the theory of elasticity, the plane strain, nonlinear, incompressible, hyperelastic (Mooney-Rivlin) finite element formulation of the software ABAQUS was used to evaluate different seal cross-sections in tension and compression with emphasis on bulge and sag and on shear strain (e_{12}). Laboratory measurements using Silicone Dow Corning 888 were taken to determine bulge and sag. It was concluded that the most desirable cross section of the three shapes is the rectangular. Axial strains (e_{11}) at the surface of the seal were compared with Tons' parabolic deformation calculations. There was good agreement all along the seal surface except near the joint walls because of a singularity. With continued research, the structural response calculations at the joint wall interface should be improved.

To make the pavement adjust to climatic conditions, joints are usually sawed or formed and a sealant material is poured or installed in the resulting groove to form a rectangular seal cross section such as the one shown in Figure 1*a*. *Wt* stands for top width; *Wb*, for bottom width; *D*, for total depth; *Dt*, for trapezoidal depth in a rectangular seal; and *Dr*, for rectangular depth in a trapezoidal-rectangular seal.

The cracking problem, however, is generally attributed to localized weakness of the pavement. These cracks are due to weather conditions (freeze-thaw cycles, large changes in temperature, shrinkage, etc.) and to loading caused by traffic.

To keep a highway in good condition and prolong its life, the cracks are sometimes grooved by a router, cleaned, then sealed. It is important to note that the resulting groove tends to have a trapezoidal shape, whether routed or not, because the top edges of a crack are exposed to weather and traffic and tend to spall because of lack of support. When a sealant material is poured into such a groove, the resulting shape of the seal may also end up being trapezoidal (Figure 1*b*), or it could be trapezoidal-rectangular (trap-rec) if there is no backup material to protect the sealant from flowing (Figure 1*c*). The problem is that cracks are sealed without trapezoidal or trap-rec cross sections being considered.

The objectives of this paper are to investigate the deformations and strains in different rubber seal cross sections (rectangular, trapezoidal, and trap-rec) using the finite element method (FEM) implemented on incompressible rubberlike materials and to compare the obtained results with laboratory measurements of top (*Ht*) and bottom (*Hb*) maximum displacements (Figure 2) with Tons' parabolic model (*1*).

M. F. Khuri, Modern Engineering Service Company, 2410 Darrow Drive, Ann Arbor, Mich. 48104. E. Tons, Department of Civil Engineering, University of Michigan, Ann Arbor, Mich. 48109.

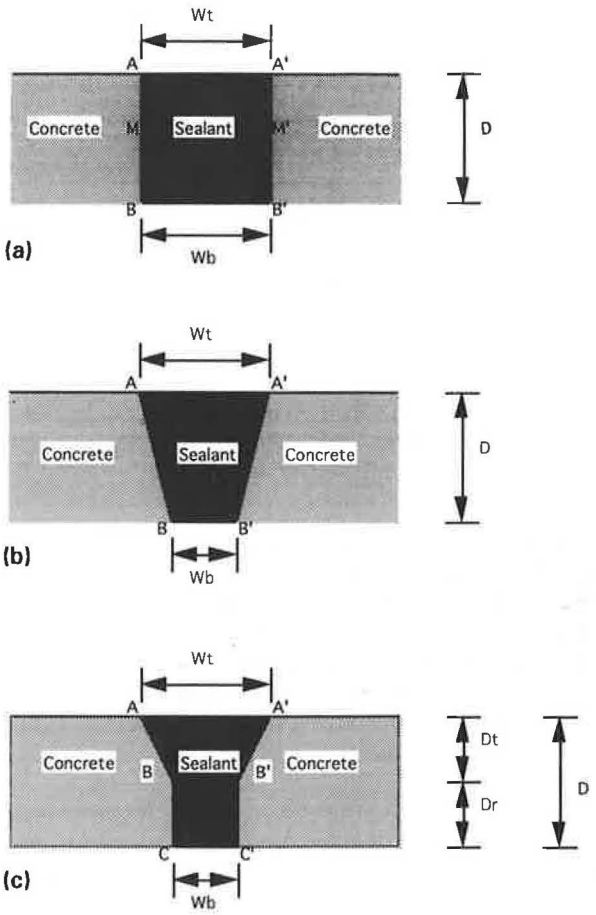

FIGURE 1 Cross sections: *a*, rectangular seal; *b*, trapezoidal seal; and *c*, trapezoidal-rectangular seal.

BACKGROUND

Rectangular Seals

The cross section of a joint is usually made rectangular. This shape is encouraged because of its simplicity (*1*).

The tools used to prepare joints for sealing and resealing are usually designed to make the joint walls vertical. The

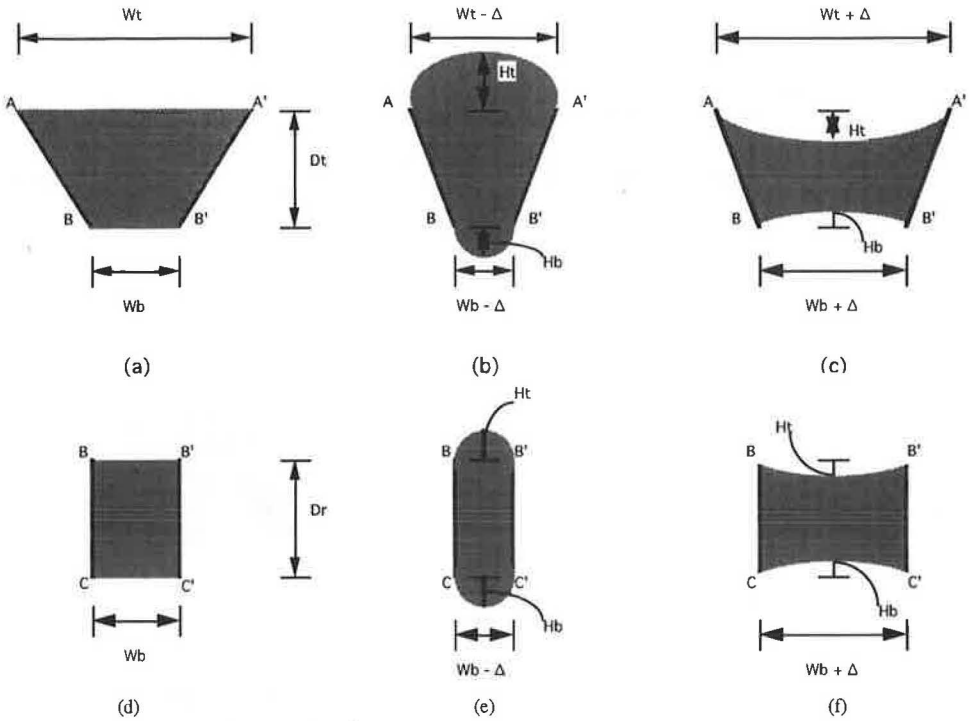

FIGURE 2 Trapezoidal seal: *a*, in its undeformed state; *b*, under compressive development; and *c*, under tensile displacement; rectangular seal: *d*, in its undeformed state; *e*, under compressive development; and *f*, under tensile displacement.

depth of the joint groove is usually controlled. Schutz (*2*) coined the term "shape factor," which has been attributed to Tons' work (*1,3*), to describe the depth-to-width ratio (*D*/*W*) of a treated joint.

A variety of sealant cross sections has been studied. Chong and Phang have experimented with a ¾- × ¾-inch cross section for transverse cracks in asphalt pavements in Canada. They also experimented with seals of dimensions 1.6 × 0.4 in. (*D*/*W* = 1/4) (*4*).

The shape factor concept for a rectangular cross section that has a *D*/*W* ratio of about 1 is generally used for sealing joints and cracks.

Trapezoidal Seals

As mentioned, trapezoidal cross sections tend to form in highway cracks because of weather and traffic. A trapezoidal cross section will also result if the crack is widened by a conical tool. Cook (*5*) mentioned that trapezoidal cross-section seals would help eliminate spalling failure in a pavement. Boot (*6*) stated that cracks do not have parallel walls like joints do, and when routed, the shape of the cross section becomes trapezoidal. Leigh (*7*), on the other hand, used trapezoidal extruded neoprene sponge rubber for cracks. The dimensions were 1- or ½-in. deep and ⅜-in. thick at the base, tapering to ¼-in. at the top.

Trapezoidal-Rectangular Seals

Trap-rec seals may exist if a crack is widened with a conical tool and not closed at the bottom by a backup rod, causing the sealant material to flow to a deeper level and making the seal cross section trapezoidal, as shown in Figure 1*c*. This cross section, as will be explained, tends to give high strains at the bottom of a seal, thereby increasing the probability of failure.

Finite Element Application

Applying the finite element method to the analysis of joint seals is a promising idea, but obtaining reliable results may be complicated. This is because rubber material used in this analysis is assumed to be incompressible, and enforcing the incompressibility condition, as far as mathematical aspects are concerned, requires special computational methods. Also, because of the large deformation encountered with sealants and the existence of a singularity, predicting the response using the classical finite element method is not very accurate. But with the use of special techniques, results can be substantially improved.

The only significant work found to have applied the finite element method to highway rubber seals was done by Wong (*8*), who used viscoelastic models. Such application is considered to be complicated, because finding the material properties and a model that predicts the behavior of the seal structure are two tedious tasks and may not be accurate. Also, the singularity at the joint-wall interface cannot be eliminated.

To analyze the response of rubberlike material, one must find the law that the material under consideration obeys. Different material laws have been suggested, such as Ogden material, Neo-Hookean material, and Mooney-Rivlin material.

The Mooney-Rivlin strain energy formulation has been used by many investigators to analyze rubberlike material (*9–15*).

The process involves determining the strain energy function of the material. Different procedures have been used to determine the strain energy function, but what is important is to fit the function to the obtained experimental data (*16–18*).

In this study the Mooney-Rivlin strain energy function was used, where material and geometric nonlinearity were assumed.

ASSUMPTIONS

Besides the fact that FEM by itself is an approximate method used in various types of structural analysis, other assumptions were made. These assumptions are as follows:

1. The material is hyperelastic, perfectly incompressible; that is, Poisson's ratio as viewed from the compressible field is equal to 0.5. This is a simplified assumption, because rubber materials in general are viscoelastic and Poisson's ratio is not exactly equal to 0.5.
2. A perfect bond is assumed between the sealant and the concrete.
3. The side at which the sealant is in contact with the concrete is assumed to be rigid or fixed in all degrees of freedom. Assumptions 2 and 3 are justified especially if the seal is handled properly (sawed, cleaned, primer is applied, and workmanship is good).
4. The sealant is assumed to be free at the bottom surface.

EXPERIMENTAL WORK

Strain Energy Function and Stress-Strain Equations

To determine the strain energy function, the use of one or more homogeneous deformations is recommended. Two homogeneous tests were used in this work, namely, simple tension and pure shear.

Specimens were prepared only with Silicone Dow Corning 888 for two main reasons:

1. Silicone Dow 888 properties do not change significantly with temperature (*19*), so it can be assumed that one strain energy function may well define the material properties at various temperature conditions—unlike rubber asphalt, for example, where one must determine the material properties at different temperatures.
2. For the same cross-sectional dimensions, FEM results for strains and displacements are the same regardless of the material type and modulus of elasticity, so it is unnecessary to do the analysis for different material properties. This is so, keeping in mind that the stresses are different but they can be normalized over the initial modulus of elasticity to give similar results for different materials.

Using the method provided in ABAQUS (*20*), which is based on minimizing the error of the function that fits both simple tension and pure shear tests, the following form of the strain energy function (U) was obtained for Silicone Dow 888:

$$U = C_1(I_1 - 3) + C_2(I_2 - 3)$$

where

$C_1 = 7.132$,
$C_2 = 7.878$,
I_1 and I_2 = first and second principal strain invariants of the left Cauchy-Green strain tensor B_{ij}, and
I_3 = third strain invariant unity (because imcompressibility condition is assumed) (*14,17*).

For a Mooney-Rivlin first-order deformation strain energy function, the stresses τ^{ij} can be obtained using the following:

$$\tau^{ij} = (2C_1 g^{ij}) + (2C_2 B^{ij}) + (PG^{ij})$$

$$g^{ij} = (g_{ij})^{-1}$$

$$G^{ij} = (G_{ij})^{-1}$$

where

$B^{ij} = (I_1 g^{ij} - g^{ir} g^{js} G_{rs})$;
g_{ij} and G_{ij} = metric tensors in undeformed and deformed configurations, respectively;
$B^{ij} = (B_{ij})^{-1}$; and
P = pressurelike variable that is calculated for every element, just like the displacement.

On the other hand, the strains ε_{ij} are of the form

$$\varepsilon_{ij} = \tfrac{1}{2}(B_{ij} - I)$$

where I is the identity matrix.

For additional and detailed explanation of the mathematical formulation and the experimental determination of the strain energy function, the reader is referred to the work by Khuri (*21*).

Determination of Top and Bottom Displacements (*Ht* and *Hb*)

Silicone Dow 888 was poured between two wood blocks that were cut to the desired dimensions. The sealant material was cast and left to cure under room temperature, then tested in the lab in tension and compression using an INSTRON machine. For a detailed description of the experimental methods, the reader is referred to the work by Khuri (*21*).

FINITE ELEMENT MODELING

Type of Element Used

Eight node elements were used throughout this study. A plane strain element called CPE8H in ABAQUS consists of eight nodes; four lie at the corners and four lie at the midpoint of each side. CPE8H is a stable element and may be best suited to model rubberlike material (*20*). The mathematical formulation of this element is explained in detail in ABAQUS (*20*) and by Khuri (*21*) and Bathe (*22*).

Number of Elements Chosen

In determining the stresses and strains in a typical seal cross section, it was observed that the response near the points A,

A', B, and B' in Figure 1*a* does not stay constant as the number of elements changes in that area (Figure 3*a*). This is because the material is fully supported at sides AB and $A'B'$ and imposing large deformation creates a discontinuity (non-Lipschitzian domain) between the material and the fixed end. This means that as one approaches the corner, the deformation tends to become tangent to the vertical axis, causing the response to increase, because the gradient tends to infinity. This means that the finite element method used is not accurate in the vicinity of the corner. However, because the objective is to compare the behavior of different seal cross sections, a model that can give values useful for comparison is needed.

It was decided to perform analyses using ABAQUS on 2-×-2, 6-×-6, 10-×-10, 20-×-20, and 80-×-80 elements. By studying the behavior of the shear strains at the integration points (Figure 3*a*), it can be observed that values are the same until the last integration point closest to the corner is reached, at which point the output of the strain is higher. Values of shear strain at the corner node versus number of elements are shown in Figure 3*b*, which shows that the value is higher for a higher number of elements and goes to infinity for an infinitely large number of elements. This again emphasizes that the finite element method does not evaluate the response accurately at the corner. However, if one finds the area under the curve in Figure 3*a* for each of the number of elements for a rectangular cross section (2 × 2, 6 × 6, 10 × 10, 20 × 20, and 80 × 80), it can be observed in Figure 3*c* that after a 10-×-10 element mesh, the area under the curve tends to be about the same regardless of the number of elements used. Because of this, it was decided to use the response that corresponds to 10-×-10 elements. These ideas were suggested by Kikuchi (*23*) and personal communications with ABAQUS consultants.

As can be observed in Figure 3*a*, if a 2-×-2 mesh is used, the shear strain obtained at the corner node may be about half of what is obtained if a 10-×-10 mesh is used. However, as the number of elements is increased, the response keeps increasing, and the upper limit tends to infinity where the $1/r$ singularity is in effect, where r is a radius that describes a domain in which, as one approaches the corner from the sealant material point of view, the stress goes to infinity.

Boundary Conditions

Modeling rectangular seals was done on the basis of 10-×-10 element mesh. After using two-directional symmetry, with respect to both x- and y-axes, a 5-×-5 element structure is obtained. All rectangular cross sections used were modeled by 5-×-5 elements regardless of the depth-to-width ratio of the seal cross section (Figure 4*a*).

Although somewhat different, both trapezoidal and trap-rec seal models may be considered under the same category and were modeled on the basis of 10-×-10 elements. After one-directional symmetry with respect to the vertical y-axis, a 10-×-5 structure was obtained. The loads and boundary conditions for trapezoidal and trap-rec cross sections are shown in Figures 4*b* and 4*c*, respectively.

RESULTS AND DISCUSSION

Comparison of Results

For the rectangular seals, laboratory results, FEM results, and the parabolic deformation model suggested by Tons (*1*) were compared. In Figure 5, Ht or Hb ($Ht = Hb$ for rectangular sections) is plotted versus extension and contraction, respectively. The legend with subscript (FE) stands for FEM results; the legend with subscript (P) stands for parabolic model results. The legend with subscript (L) stands for laboratory results. Note that laboratory results for each specimen size are based on the average of results obtained from three specimens. Similar results were obtained when comparing laboratory results and FEM results for trapezoidal and trap-rec cross sections. Figure 5 shows that the experimental measurements are close to FEM results (range between 2 to 10 percent difference), and Tons' calculations tend to overestimate the measurements (range up to about 20 percent difference).

Comparisons Based on FEM Only

It is important to note that using the finite element method, the top and bottom displacements obtained from similar specimen dimensions gave the same top and bottom displacements and strains regardless of the material properties. This behavior is expected, because the material is considered incompressible (it deforms with no change in volume); the deformation should be the same, regardless of the modulus of elasticity of the material. This is true, even though the force required to stretch different materials to the same amount of displacement may be different, but the force can be normalized over the modulus of elasticity to give similar results.

In the following subsections, the behavior of rectangular, trapezoidal, and trap-rec seal cross sections under tensile and compressive displacements was investigated for typical selected specimens. Variations of strains and displacements in the seal structures are reported.

Comparison of Displacement (Ht *and* Hb)

In comparing rectangular, trapezoidal, and trap-rec rubber seal cross sections, it is important to understand the mechanism of deflection, in tension and in compression. In this paper, tensile displacements are emphasized. For a more detailed description of the performance under compressive displacements, see Khuri (*21*).

A trapezoidal cross section, which is the top portion of a trap-rec section, is shown in Figure 2*a* in its undeformed state; in Figure 2*c*, it is shown under tensile displacement. A rectangular cross section, which is the bottom portion of a trap-rec seal, is shown in Figure 2*d* in its undeformed condition; in Figure 2*f*, it is shown under tensile displacement. Note that Ht and Hb are identical because of symmetry. However, in Figure 2*c*, which shows a trapezoidal seal under tensile displacement, Ht is always greater than Hb. For trap-rec cross sections, behavior can not be predicted without calculations (Ht may be larger or smaller than Hb, as will be explained

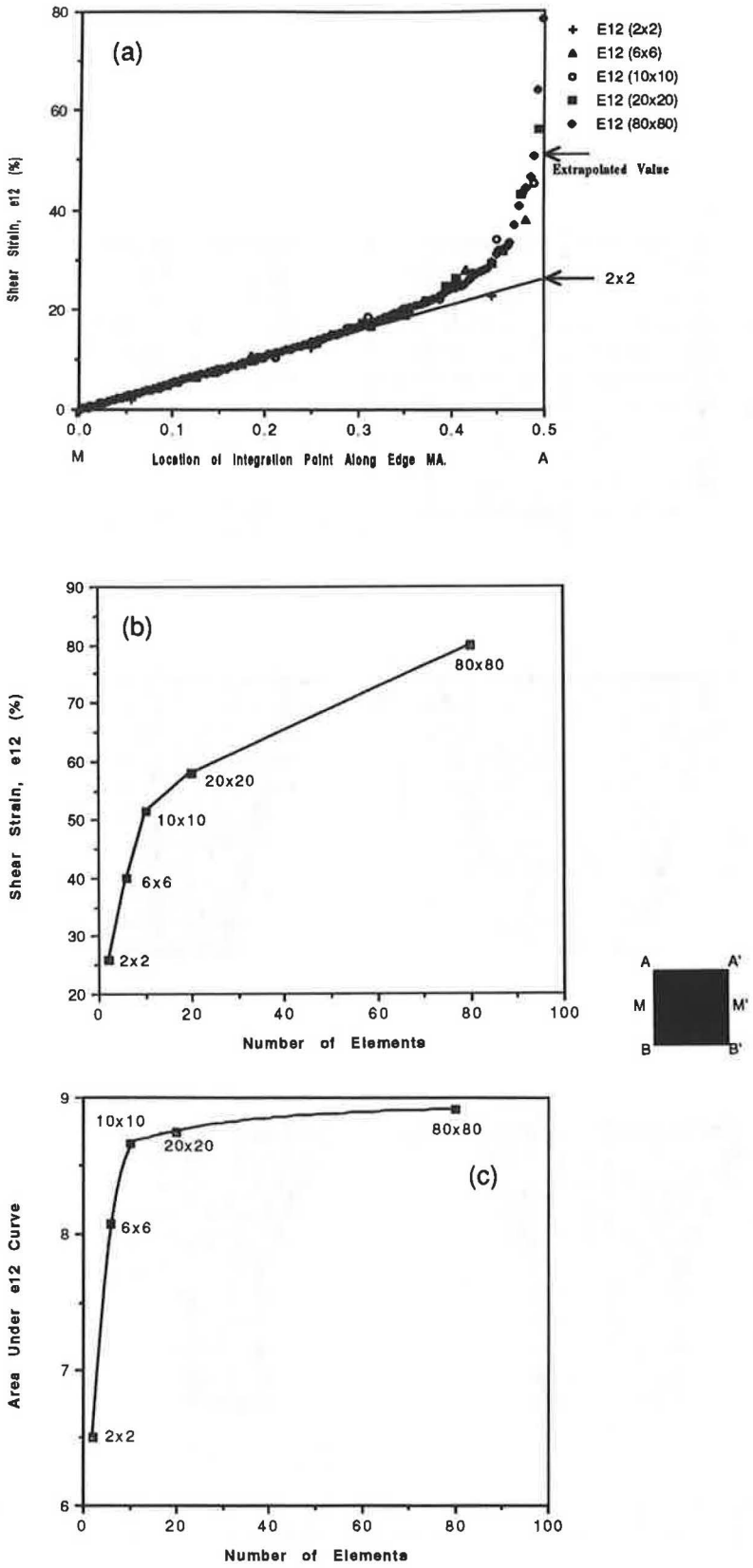

FIGURE 3 Evaluation of finite element model: *a*, shear strain versus location of corresponding integration points between *M* and *A* at 20 percent *Wb* tensile displacement; *b*, shear strain at corner node versus number of elements; and *c*, area under shear strain curve versus number of elements in FEM model.

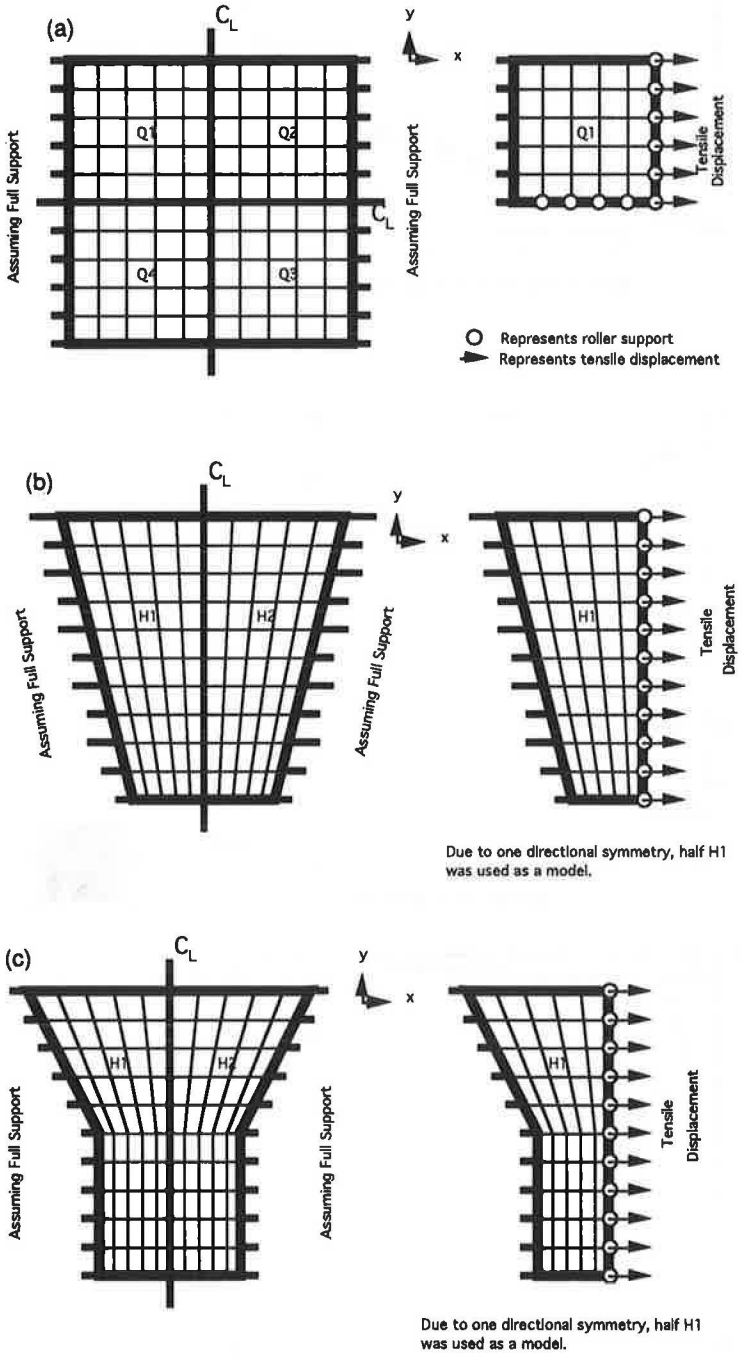

FIGURE 4 Finite element model: *a*, rectangular cross section; *b*, trapezoidal cross section; and *c*, trapezoidal-rectangular cross section.

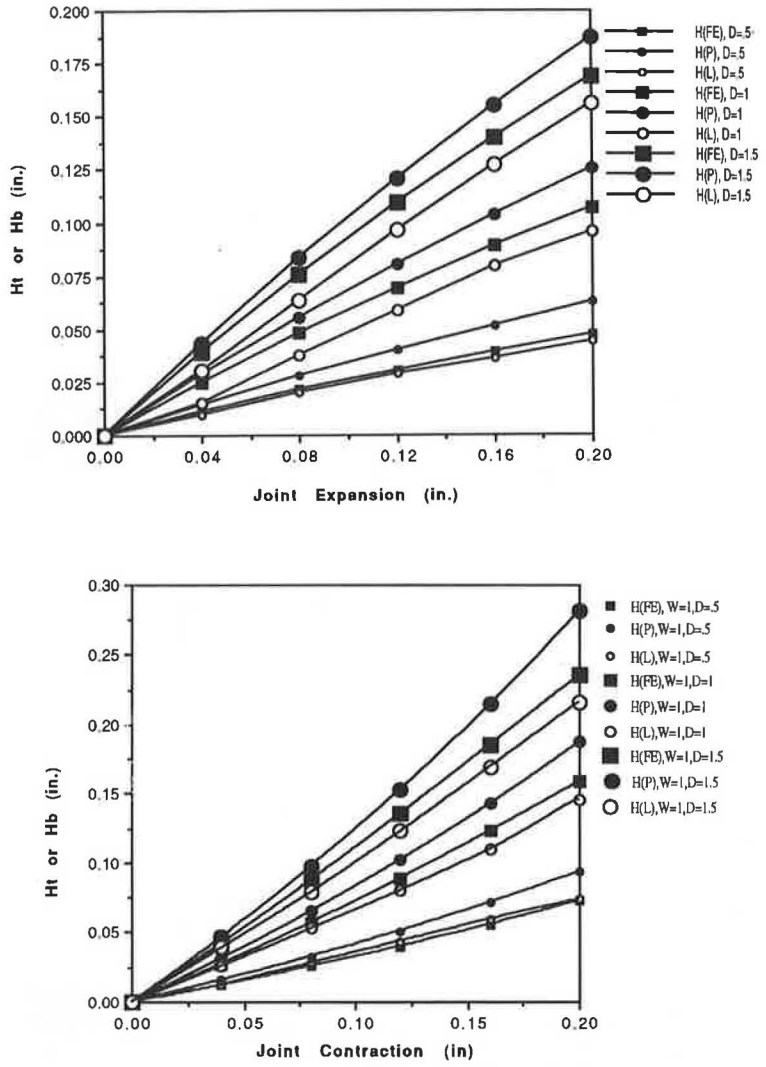

FIGURE 5 Comparison between lab, parabolic, and FEM results for Ht or Hb versus extension (*top*) and contraction (*bottom*) for different rectangular cross sections.

later). The same principle applies to seals under compressive displacement shown in Figures 2*b* and 2*e*.

Comparisons Based on Strains

In this section, strains in the x-direction (e_{11}), strains in the y-direction (e_{22}), and shear strains (e_{12}) are evaluated for all three cross sections.

Edge Conditions For all seal cross sections, edge conditions along Line ABC in Figure 1*c* yielded the highest shear strains. This is due to stress concentration near the corner. In this region, only the shear strain was considered because all other strains are zero at a fixed edge. Some values were obtained for e_{11} and e_{22} at the corners and along the edge, because in finite element analysis, response is calculated at integration points and then extrapolated to the nodes.

Shear strain (e_{12}) versus location along the depth as shown in Figure 6 is drawn at the edge for rectangular, trapezoidal, and trap-rec cross sections.

Figure 6*c* shows the shear strain behavior in a trap-rec cross section under 20 percent of Wb tensile displacement. It starts from depth equal zero at the bottom to depth equal one at the top. Shear strain (e_{12}) is highest at the bottom corner. Going up from the bottom corner, e_{12} decreases until the midline is reached, which is the point at which the rectangular cross section ends and the trapezoidal cross section starts. At this point there is a strain concentration, and on the way up toward the trapezoidal portion, the strains decrease because the imposed displacement on the seal is only 20 percent of Wb, which is 5 percent of Wt.

Figure 6*b* is plotted for e_{12} at the edge from bottom to top for a trapezoidal cross section. Shear strains are highest at the bottom, decrease to zero at about quarter of the depth going up, then increase again at the top, because of the corner.

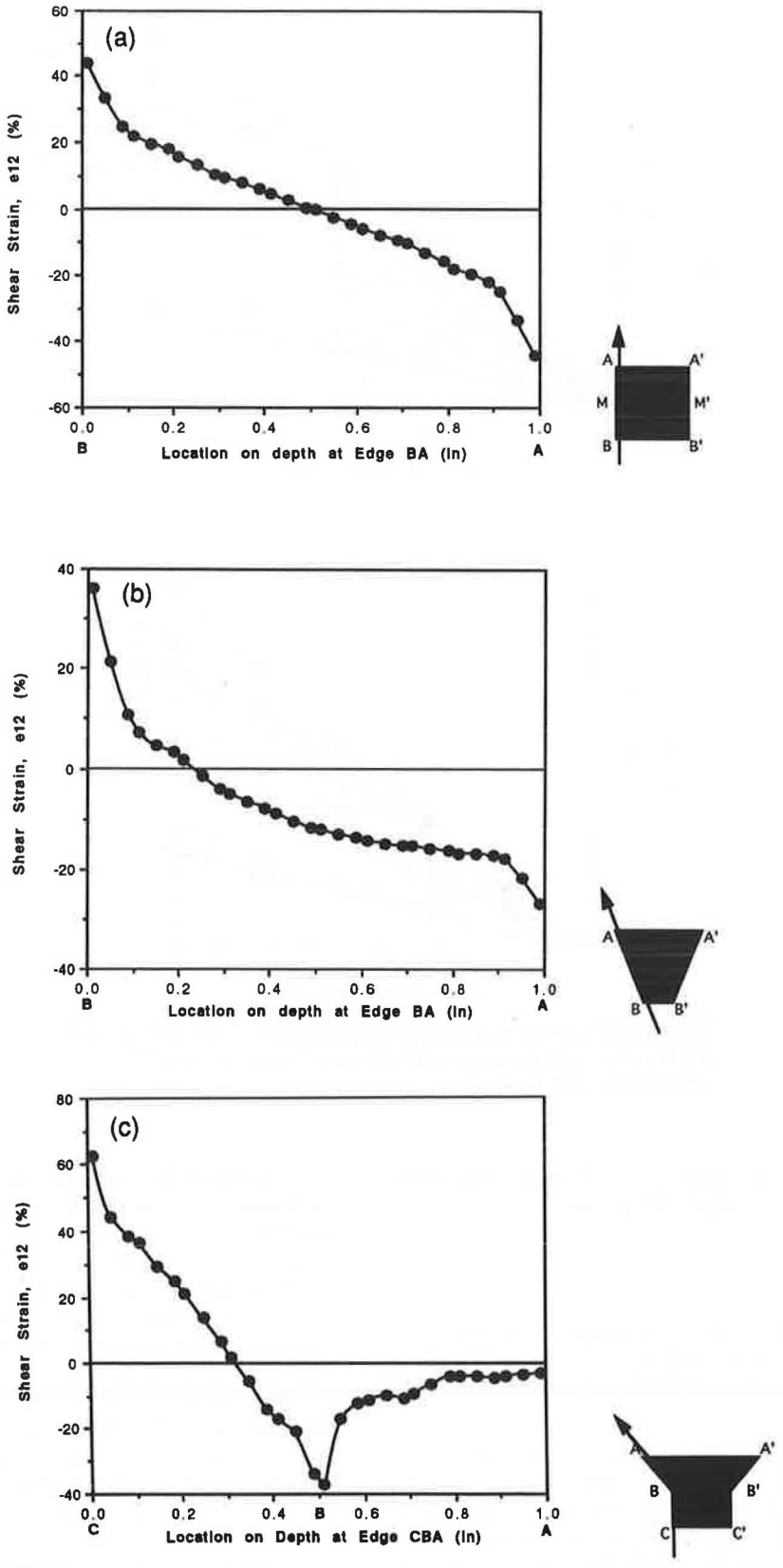

FIGURE 6 Shear strain versus location of integration points at 20 percent *Wb* tensile displacement for $D = 1$ and $Wt = 1$: *a*, shear strain along Line *BA* for seal cross section $Wb = 1$; *b*, shear strain along Line *BA* for seal cross section $Wb = 0.5$; and *c*, shear strain along Line *CBA* for seal cross section $Wb = 0.25$ and $Dr = 0.5$.

In Figure 6*a*, e_{12} is highest at the bottom or top corner, decreasing to zero at the center, and then increasing to a maximum at the other corner. Note that values at both corners are equal due to symmetry.

Centerline Conditions In Figure 7, e_{11}, e_{22}, and e_{12} are plotted at the centerline of symmetry with respect to the *y*-axis. Very consistent results are observed where e_{11} and e_{22} are equal and opposite in magnitude because the volumetric strain is zero. That is to say, since the total volumetric strain, $e_{11} + e_{22} + e_{33} = 0$, and $e_{33} = 0$, $e_{11} = -e_{22}$. On the other hand, e_{12} is always about zero at the center.

Comparison of e_{11} with Parabolic Model Figure 8 shows axial strain (e_{11}) comparison between FEM results and the results obtained by Tons' parabolic model for a rectangular cross section along Line *AA'* and *BB'* (*1*). It can be observed that e_{11} is uniform in magnitude in the interior portion of the seal, and there is an agreement in results between Tons' model and FEM all along the seal surface except at the corners of the joint-wall interface.

Effects of Variations in Cross-Section Dimensions

In the following analysis and discussion, a typical trap-rec cross section was used as the starting point with varied dimensions. Rectangular and trapezoidal cross sections were covered in the analyses of these variations.

Effects of Variations in Bottom Width (Wb)

A trap-rec cross section was analyzed for different values of *Wb*, keeping *Wt*, *Dt*, and *Dr* constant. *Wb* was varied between ⅛ and 1 in. at *Wt* = 1, *Dt* = 0.5, and *Dr* = 0.5 in. Graphs for the shear strains and maximum displacements versus *Wb* are shown in Figure 9.

It can be noticed from Figure 9 (*top*) that there is a significant increase in shear strain between values at *Wb* = 1 and values at *Wb* = ⅛ in. At 20 percent of *Wb* displacement, e_{12} at *Wb* = 0.125 is about 1.6 e_{12} at *Wb* = 1.

In Figure 9 (*bottom*), *Ht* and *Hb* are plotted against *Wb*. Note that the maximum *Ht* at *Wb* = 1 is about 3 times higher than the maximum *Ht* when *Wb* = ⅛ in. This may be because the structure is being displaced to 20 percent of *Wb*. When *Wb* = ⅛ in., the total imposed 20 percent *Wb* displacement is 0.025; when *Wb* = 1 in. the total displacement is 0.2, which is eight times larger.

Note also that *Ht* is less than *Hb* at values of *Wb* < 0.35 in. and becomes greater between values of 0.35 ≤ *Wb* < 1. At *Wb* = 1, the section is rectangular or square and *Ht* = *Hb*. This behavior might be explained as follows: when the seal is very narrow at the bottom rectangular portion, the 20 percent extension of *Wb* is small compared with *Wt* and does not have a significant effect on the trapezoidal portion.

Effects of Variations in Rectangular Depth (Dr)

The same trap-rec cross section was analyzed for different values of *Dr*, keeping *Wt*, *Wb*, and *Dt* constant. *Dr* was varied between 0 and 1.5 in. Graphs for the shear strains and maximum displacements versus *Dr* are shown in Figure 10.

It can be observed in Figure 10 (*top*) that as *Dr* increases, maximum shear strain increases significantly. That is, e_{12} for *Dr* = 1.5 is about seven times e_{12} for *Dr* = 0. This means that if the crack were closed at the bottom of the trapezoidal section, the strain concentration could be decreased seven times.

Figure 10 (*bottom*) shows *Ht* and *Hb* at 20 percent of *Wb* displacement. *Hb* at *Dr* = 1.5 is about 20 times higher than when *Dr* = 0, that is, when the section is only trapezoidal.

It is important to observe that although the top width is wider than the bottom width, it can be seen that *Hb* at high *Dr* > 0.35 tends to be larger than *Ht*, making *Ht*/*Hb* < 1. As the rectangular depth *Dr* increases, both displacements increase. As *Dr* reaches about 0.35, *Hb* becomes greater than *Ht*.

Effects of Variations in Trapezoidal Depth (Dt)

Again, the same trap-rec cross section was analyzed for different values of *Dt*, keeping *Wt*, *Wb*, and *Dr* constant. *Dt* was varied between 0 and 1.5 in. at constant *Wt* = 1, *Wb* = 0.25, and *Dr* = 0.5 in. Results show that *Dt*, when compared with *Dr* or *Wb*, does not have a significant effect on the change in response. For detail explanations, the reader is referred to the work by Khuri (*21*).

GENERAL OBSERVATIONS

The discussion shows that as *Dr* of a trap-rec section increases, strains, *Ht*, and *Hb* increase significantly and that as *Wb* decreases, the response increases accordingly.

In comparing Figures 9 and 10, it can be observed that an increase in *Dr*, as seen in Figure 10, has a significantly larger effect on the increase in shear strain (e_{12}) and displacements (*Ht* and *Hb*) than that of a decrease in *Wb* in Figure 9. This is because an increase in the depth of a narrow joint (*Wb* = 0. 25) will increase the strains, because when *Dr* = 1.5, larger deformations will occur in the material near the bottom corner.

Also, the displacement imposed on the sealant is 20 percent of *Wb* throughout. If this crack were actually designed or assumed to be larger than the actual *Wb*, then a 20 percent displacement would give much higher values because it is not 20 percent anymore, but actually it could be 50 or 100 percent. If a crack is assumed to be ½-in. at the bottom and was designed or expected to be such, then 20 percent of *Wb* is equal to 0.1 in. However, if the crack is not closed at the bottom, the material will flow into a much smaller *Wb* than was calculated for—say, ⅛ in. This means that a 0.1-in. displacement is not 20 percent of *Wb* anymore but 80 percent of *Wb*. A displacement of 80 percent of *Wb* would cause very large strains in a seal.

As can be seen from these results, closing the bottom of the joint may improve the performance and life expectancy of crack sealants. This can be done by installing a special backup rod at the desired depth.

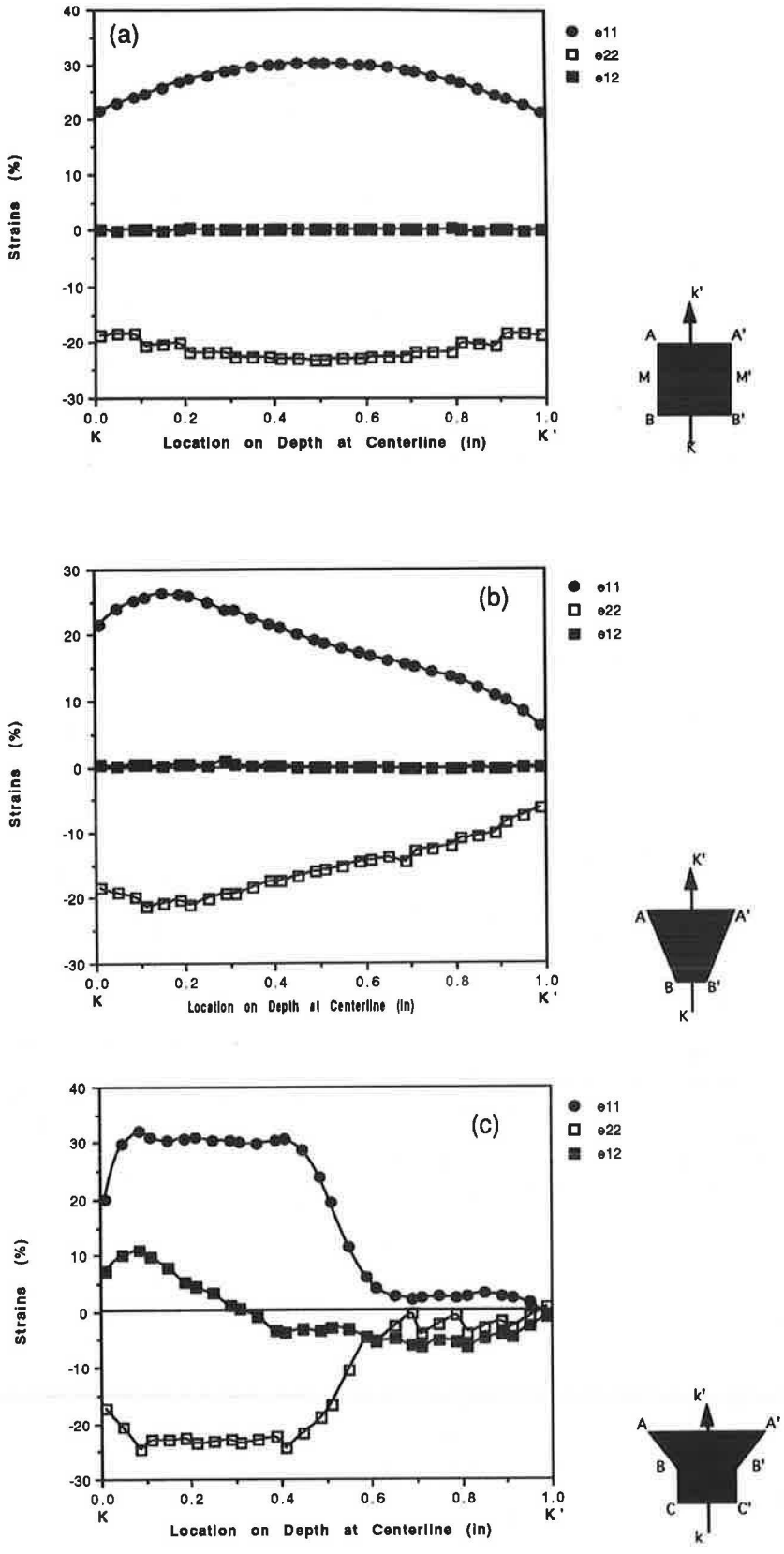

FIGURE 7 Strains versus location of integration points at 20 percent *Wb* tensile displacement for $D = 1$ and $Wt = 1$: *a*, strains along Line *KK'* for seal cross section $Wb = 1$; *b*, strains along Line *KK'* for seal cross section $Wb = 0.5$; and *c*, strains along Line *KK'* for seal cross section $Wb = 0.25$, $Dt = 0.5$, and $Dr = 0.5$.

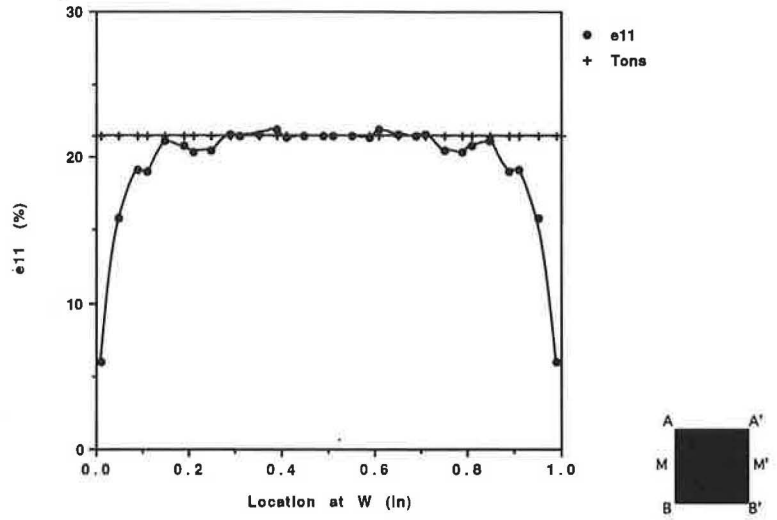

FIGURE 8 Surface strain (e_{11}) comparison between FEM results and Tons' parabolic model calculations along line *AA'* or *BB'* for a rectangular seal.

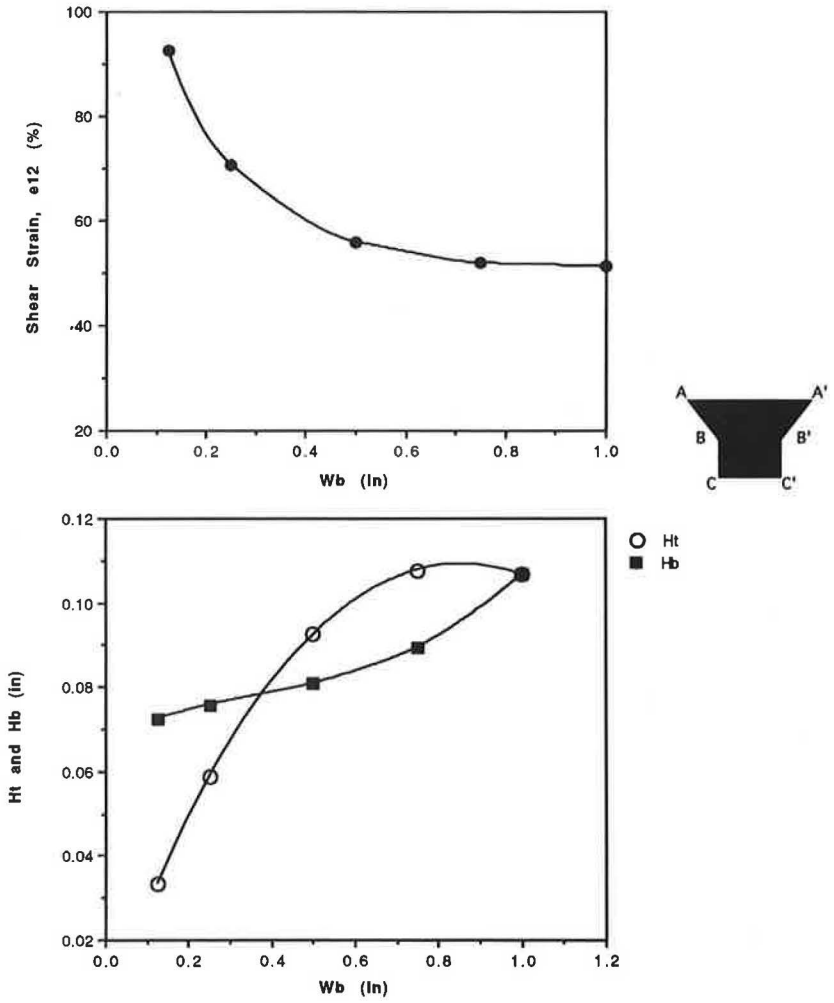

FIGURE 9 Evaluation of shear strains (e_{12}) and *Ht* and *Hb* versus changes in bottom width *CC'* for trap-rec seal at 20 percent *Wb* tensile displacement for constant *Wt* = 1, *Dt* = 0.5, and *Dr* = 0.5: *top*, shear strain versus *Wb*; *bottom*, *Ht* and *Hb* versus *Wb*.

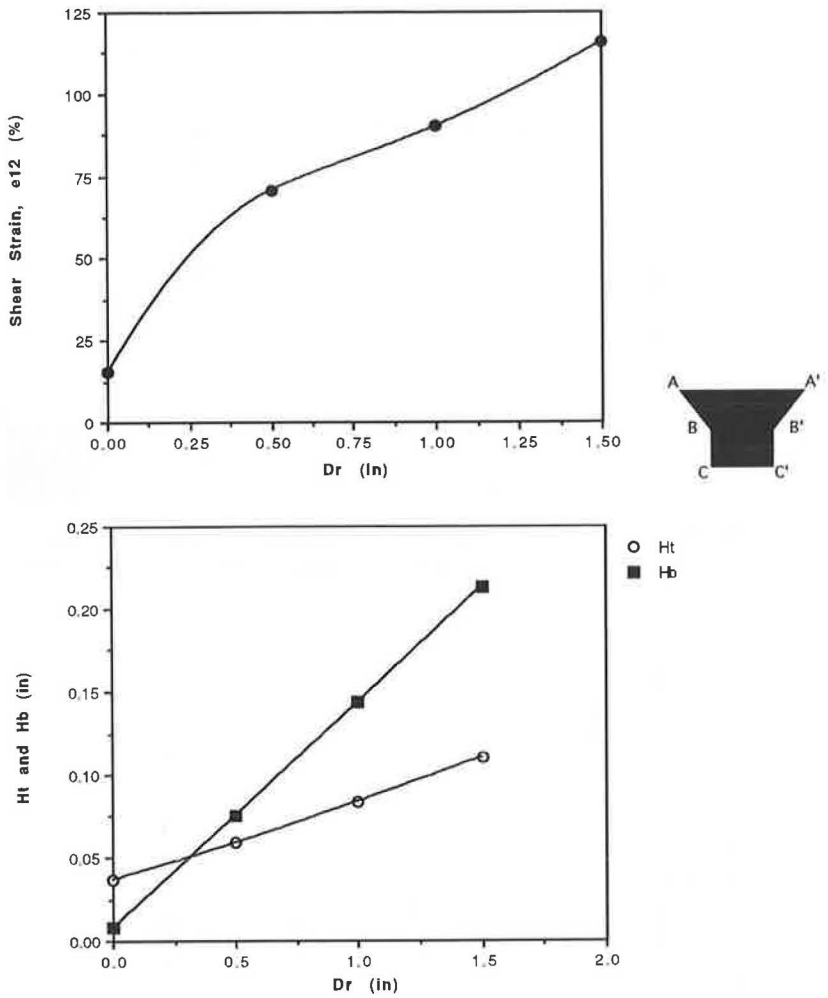

FIGURE 10 Evaluation of shear strains (e_{12}) and *Ht* and *Hb* versus changes in bottom width *CC'* for a trap-rec seal at 20 percent *Wb* tensile displacement for constant *Wt* = 1, *Wb* = 0.5, and *Dt* = 0.5: *top*, shear strain versus *Dr*; *bottom*, *Ht* and *Hb* versus *Dr*.

CONCLUSIONS

Laboratory measurements and nonlinear incompressible hyperelastic (Mooney-Rivlin) finite element formulations were used to compare different seal cross sections. Silicone Dow 888 was used for laboratory determination of the strain energy function and bulge and sag measurements. Using certain assumptions, finite element analysis was used to calculate strains and displacements. Comparisons between all cross sections were made on the basis of strains and displacements and cross-sectional variations in dimensions.

It was concluded that

1. The most desirable cross section is rectangular, because trapezoidal and trap-rec cross sections can cause high strains if not properly designed and implemented.
2. Wide and shallow seals are highly recommended; seals with a high *W/D* ratio (> 1.5) provide lower strains than those with a low *W/D* ratio.
3. $Ht = Hb$ for rectangular cross sections and $Ht > Hb$ for trapezoidal cross sections, but *Ht* and *Hb* for a trap-rec cross section are not predictable without calculations and depend mostly on *Dr* and *Wb*.
4. As the bottom width (*Wb*) in a trapezoidal seal is decreased and the depth is increased, strains are increased; as the material is allowed to flow deeper into a crack, it creates a point of high stress concentration. This leads to the conclusion that cracks should be closed at the bottom by a backup rod to eliminate the possibility of creating a trap-rec cross section.
5. Tons' parabolic calculations (for rectangular seals) and the finite element analysis appear to be in close agreement for the maximum displacements, bulge and sag. For the axial strain (e_{11}), results show that there is a good agreement all along the sealant surface except at the corners, where the sealant meets the joint walls. Tons' method does not apply to trapezoidal or trap-rec cross sections.
6. The FEM method used in this research seems to be promising, but it did not accurately predict the response at the corners because of a discontinuity. However, with continued research and development in this area, improvements may be expected, including new seal design procedures.

RECOMMENDATIONS

Recommendations for future research are summarized as follows:

1. Experimentally determine failure strain limit inside the seal by implanting strain gauges at the corners and throughout the seal structure and simulating environmental conditions; using these values, comparison with FEM results can be made.
2. Apply the theory of fracture mechanics to determine bond failure criteria, then use the polynomial version of the finite element method, which may be more stable at the discontinuity.

ACKNOWLEDGMENT

This paper is part of a Ph.D. thesis written by M. F. Khuri at the University of Michigan, Ann Arbor.

REFERENCES

1. E. Tons. A Theoretical Approach to the Design of a Road Joint Seal. *Bulletin 229*, HRB, National Research Council, Washington, D.C., 1959, pp. 20–53.
2. R. J. Schutz. Shape Factor in Joint Design. *Civil Engineering*, Vol. 32, No. 10, 1962, pp. 32–36.
3. E. Tons. Field Molded Joint Seal in Tension and Compression. *Joint Sealing and Bearing Systems for Concrete Structures*. Special Publication 94. American Concrete Institute, 1986.
4. G. J. Chong and W. A. Phang. *Improved Preventive Maintenance: Flexible Pavements in Cold Regions*. Research Report 8. Research and Development Branch, Ministry of Transportation and Communications, Ontario, Canada, 1988.
5. J. P. Cook. A Study of Polysulfide Sealants for Joints in Bridges. In *Highway Research Record 80*, HRB, National Research Council, Washington, D.C., 1965, pp. 11–35.
6. R. J. Boot. Sealants. *Silicone Sealants* (A. Damusis, ed.), Reinhold Publishing Co., New York, N.Y., 1967, Chapter 4.
7. J. V. Leigh. Repairing Cracked Concrete Road Slabs. *Road and Road Construction*, Jan. 13, 1965.
8. C. J. Wong. *A Finite Element Analysis of Viscoelastic Sealants*. Ph.D. thesis. University of Cincinnati, Ohio, 1984.
9. M. Mooney. The Theory of Large Elastic Deformations. *Journal of Applied Physics*, Vol. 11, 1940, pp. 522–530.
10. R. S. Rivlin and D. W. Saunders. Large Elastic Deformations of Isotropic Materials: VII. Experiments on the Deformation of Rubber. *Philosophical Transactions*, Series A, No. 243, 1950, pp. 251–288.
11. L. R. G. Treloar. *The Physics of Rubber Elasticity*. Oxford University Press, London, England, 1958.
12. A. E. Green and J. E. Atkins. *Large Elastic Deformations (and Non-linear Continuum Mechanics)*. Oxford University Press, London, England, 1960.
13. C. Truesdell and W. Noll. The Non-linear Field Theories of Mechanics. *Encylopedia of Physics* (S. Fluegge, ed.), Vol. 3. Springer-Verlag, Berlin, Germany, 1965.
14. A. E. Green and W. Zerna. *Theoretical Elasticity*, 2nd ed. Oxford University Press, London, England, 1968.
15. R. W. Ogden. Large Deformation Isotropic Elasticity—On the Correlation of Theory and Experiment for Incompressible Rubber-like Solids. *Proc., Royal Society of London*, Series A, No. 326, 1972, pp. 565–585.
16. B. G. Kao and L. Razgunas. *On the Determination of Strain Energy Function of Rubbers*. Ford Motor Company, 1987.
17. R. E. Marusak. *Determining the Parameters of Elastic Strain Energy Equations*. Report 88–04. The Texas Institute for Computational Mechanics, University of Texas, Austin, May 1988.
18. T. Scharnhorst and H. H. Pian. Finite Element Analysis of Rubber-like Materials by a Mixed Model. *International Journal of Numerical Methods for Engineering*, Vol. 12, 1978, pp. 665–676.
19. S. Spells and J. M. Klosowski. *The Importance of Sealant Modulus to the Long-Term Performance of Concrete Highway Joint Sealants*. Dow Corning Corp.
20. *ABAQUS (Finite Element Program)*, Version 4. Hibbitt, Karlsson and Sorensen, Inc., Providence, R.I., 1987.
21. M. F. Khuri. *Analysis and Design of Incompressible Rubber Seals Using Experimental and Finite Element Methods*. Ph.D. thesis. Department of Civil Engineering, University of Michigan, Ann Arbor, Dec. 1989.
22. K. J. Bathe. *Finite Element Procedures in Engineering Analysis*. Prentice-Hall, Englewood Cliffs, N.J., 1982.
23. N. Kikuchi. *Finite Element Methods in Mechanics*. Cambridge University Press, New York, N.Y., 1986.

Publication of this paper sponsored by Committee on Sealants and Fillers for Joints and Cracks.